

Original Research Article

IN-SILICO EVALUATION OF PHENYLISOCYTOSINE AND ITS ANALOGS AS POTENT INHIBITORS OF PLASMODIUM FALCIPARUM TRANSKETOLASE: A STRATEGIC APPROACH IN ANTI-MALARIAL DRUG DISCOVERY

ABSTRACT

Background: The rise of drug-resistant *Plasmodium falciparum* strains, particularly those resistant to artemisinin-based combination therapies (ACTs), underscores the urgent need for alternative antimalarial agents targeting novel biochemical pathways.

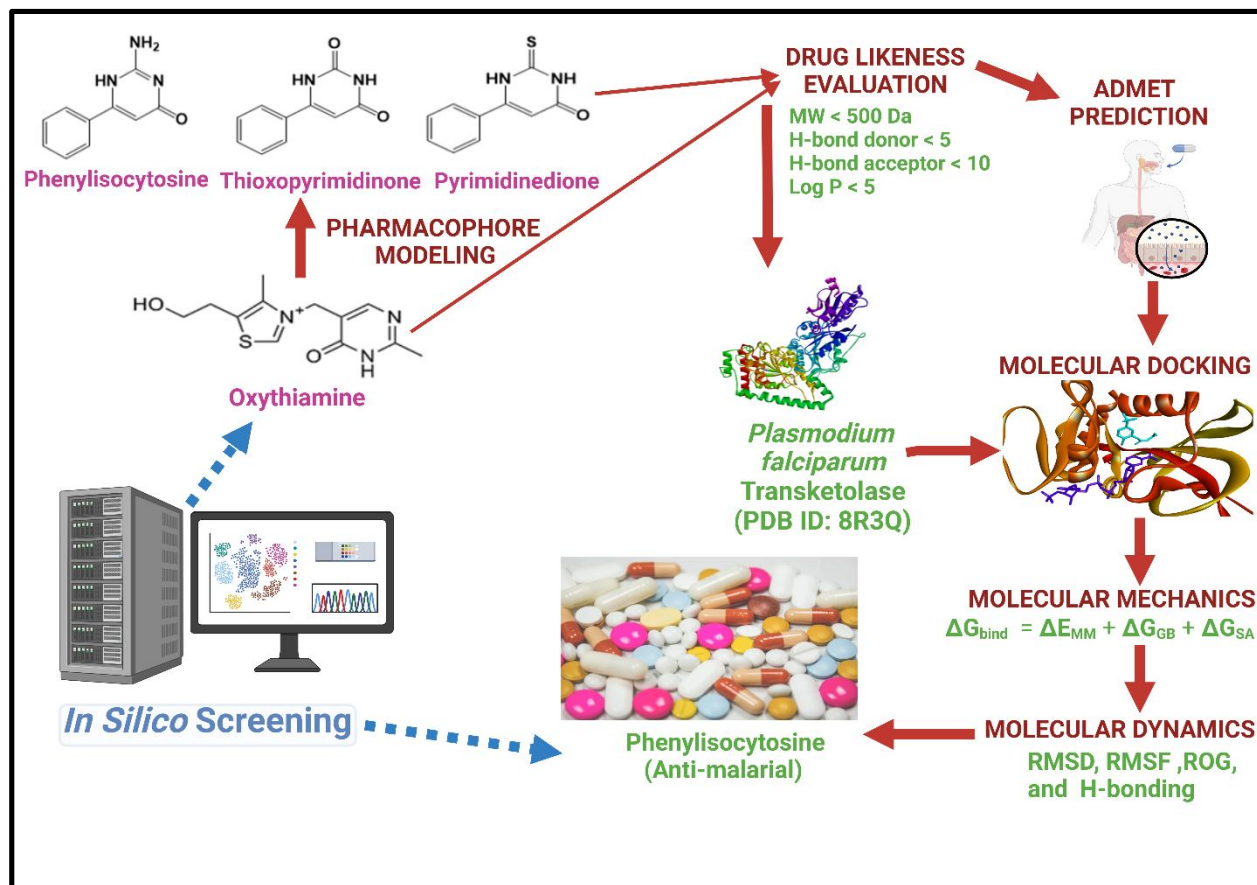
Aim: This study investigates the potential of pyrimidine-based compounds (phenylisocytosine, thioxopyrimidinone, and pyrimidinedione) as potential inhibitors of transketolase, a critical enzyme in the pentose phosphate pathway essential for parasite nucleotide synthesis and redox homeostasis.

Methodology: Selected for their structural similarity to oxythiamine—a potent but nephrotoxic and carcinogenic transketolase inhibitor—these compounds were modified to improve safety profiles while retaining inhibitory efficacy. Using a combination of ligand-based and structure-based drug design approaches, comprehensive *in silico* assessments were conducted.

Results: Pharmacokinetic evaluations, including drug-likeness and ADMET profiling, indicated favorable drug-like properties and low toxicity across all compounds. Molecular docking studies identified phenylisocytosine as having the highest binding affinity with *Plasmodium falciparum* transketolase (-6.3 kcal/mol in AutoDock Vina and -8.5 kcal/mol in iGEMDock), outperforming both thioxopyrimidinone and pyrimidinedione. Molecular mechanics calculations confirmed phenylisocytosine's superior binding free energy (-26.05 kcal/mol), with the reference drug oxythiamine exhibiting the weakest interaction (-16.85 kcal/mol). Molecular dynamics simulations over 50 nanoseconds further validated phenylisocytosine as the most stable ligand in complex with *Plasmodium falciparum* transketolase, with an RMSD of 0.30 nm, RMSF of 0.12 nm, ROG of 3.01 nm, and H-bond length of 1.01 nm. Although thioxopyrimidinone and oxythiamine showed moderate stability, phenylisocytosine consistently excelled across all parameters.

Conclusion: These findings position phenylisocytosine as a promising candidate for further preclinical studies, presenting a potential new approach to addressing antimalarial drug resistance.

GRAPHICAL ABSTRACT



Keywords: Antimalarial resistance, *Plasmodium falciparum* transketolase, Oxythiamine, Phenylisocytosine, Ligand-based drug design, Structure-based drug design.

1.0 INTRODUCTION

Malaria remains a major global health challenge, particularly in tropical and subtropical regions, where *Plasmodium falciparum* has developed resistance to existing antimalarial therapies. The widespread emergence of resistance to artemisinin-based combination therapies (ACTs), which have been the standard for malaria treatment over the past decades, underscores the urgent need for new therapeutic approaches to combat drug-resistant strains.^[1,2] Despite significant advances in reducing malaria mortality, the World Health Organization (2023) still reports a substantial number of malaria-related deaths each year, particularly in areas where drug resistance is prevalent.^[3] Historically, antimalarial drugs such as quinine and chloroquine played crucial roles in malaria control, but resistance to these therapies, and now ACTs, has driven the need to identify alternative drug targets within *Plasmodium falciparum* to develop effective treatments.^[4,5]

One promising avenue in the search for alternative antimalarial therapies involves targeting the pentose phosphate pathway (PPP), a critical metabolic pathway in *Plasmodium falciparum* responsible for nucleotide synthesis and maintaining redox balance, which are essential for parasite survival. Within the non-oxidative branch of the PPP, *Plasmodium falciparum* transketolase has emerged as a viable therapeutic target, as its inhibition disrupts key metabolic processes, potentially hindering parasite development and survival.^[6,7] This study investigates the inhibitory potential of phenylisocytosine and its analogs—thioxypyrimidinone and pyrimidinedione—against *Plasmodium falciparum* transketolase. These compounds are structurally related to oxythiamine, a known transketolase inhibitor; however, modifications were made to improve their safety profiles by reducing adverse effects associated with oxythiamine, such as nephrotoxicity and carcinogenicity, making them suitable candidates for antimalarial drug development.^[8]

Recent advancements in computational drug discovery have transformed the early stages of antimalarial drug design by enabling accurate predictions of ligand-receptor interactions, binding affinities, and pharmacokinetic properties. Structure-based drug design (SBDD) and ligand-based drug design (LBDD) are now widely employed for screening potential inhibitors and optimizing lead compounds for further development.^[9,10] Using these computational techniques, molecular docking, molecular mechanics, and molecular dynamics simulations allow for a comprehensive evaluation of a compound's binding efficiency, stability, and dynamic behavior within the target protein.^[11] In this study, phenylisocytosine and its analogs were rigorously assessed using *in silico* methods, including pharmacokinetic profiling with Lipinski's Rule of Five and ADMET (Absorption, Distribution, Metabolism, Excretion, and Toxicity) analysis, to determine their suitability for further preclinical exploration.

The identification of phenylisocytosine and its analogs as potential inhibitors of *Plasmodium falciparum* transketolase represents a promising strategy for overcoming antimalarial drug resistance. Comprehensive *in silico* evaluations in this study offer crucial insights into these compounds' interaction dynamics with *Plasmodium falciparum* transketolase and support their advancement to future preclinical studies. By focusing on alternative metabolic pathways, specifically the non-oxidative branches of the PPP, this approach provides a strategic advantage in targeting drug-resistant malaria strains. The findings not only highlight the therapeutic potential of phenylisocytosine and its analogs but also underscore the importance of exploring alternative metabolic targets to address the persistent challenge of malaria treatment.^[12]

2.0 METHODOLOGY

2.1 Preparation of target protein and determination of active site.

The essential information on *plasmodium falciparum* transketolase was obtained via the Protein Data Bank (PDB) (<https://www.rcsb.org>). The homo-domain three-dimensional structure of transketolase from *plasmodium falciparum* as a receptor was utilized as the receptor for this study, with particular focus on its domain D (PDB ID: 8R3Q) with a resolution of 1.88 Å (<https://doi.org/10.2210/pdb8r3q/pdb>). Biovia Discovery Studio 2021 (<http://www.accelrys.com>) was employed to optimize the protein structure, ensuring no unintended interactions affected the virtual screening process. The active site of the target protein was predicted using the CASTp 3.0 web server, a widely recognized tool for accurately identifying potential drug interaction sites, which facilitated precise, site-specific docking.^[13]

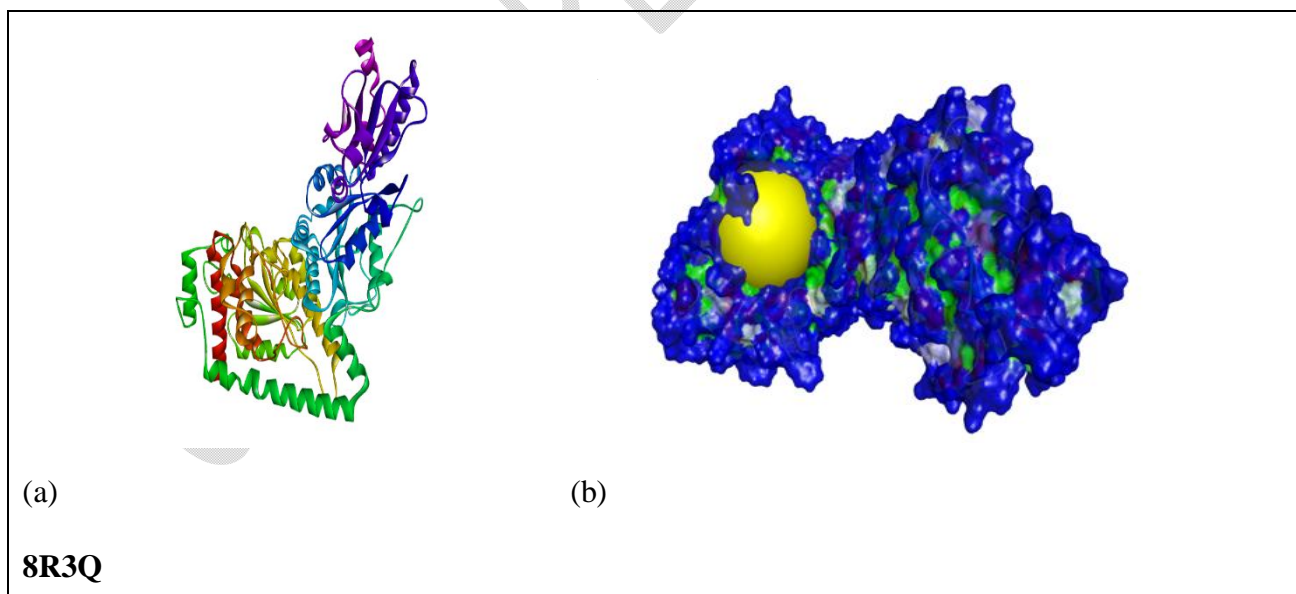


Figure 1: Visualization of *plasmodium falciparum* transketolase receptor (PDB ID: 8R3Q), (a) cartoon model (b) surface model with the active site colored in yellow.

2.2 Preparation of Ligands

This *in silico* study focused on phenylisocytosine and its analogs, which were evaluated as potential antimalarial agents. Oxythiamine, used as a reference drug, was obtained from the PubChem database (<https://pubchem.ncbi.nlm.nih.gov/>). Pharmacophore modeling of oxythiamine was conducted using the ZINC20 database (<https://zinc20.docking.org/>), yielding phenylisocytosine, thioxopyrimidinone, and pyrimidinedione. These structures were optimized in 3D using ACD/Chemsketch version 2018 (<http://www.acdlabs.com/>) and saved in PDB format. All compounds were converted to PDBQT format using Open Babel^[14], to enable interaction studies with the target protein, facilitating a detailed examination of binding interactions.

2.3 Molecular Docking Validation

To increase the accuracy of virtual screening, consensus scoring was implemented using AutoDock Vina, iGEMDock, and Molecular Operating Environment, each utilizing distinct algorithms.^[15-17] These tools assessed the binding affinity and interactions of the co-crystallized ligand, thiamine pyrophosphate, within the D-domain active site of *Plasmodium falciparum* transketolase. AutoDock Vina and iGEMDock produced comparable binding scores and structural conformations, making them suitable for the primary docking phase. This consensus scoring minimized false positives and negatives, ensuring reliable predictions of potential drug efficacy.

2.4 Physicochemical, Pharmacokinetic and Toxicological Profiling.

2.4.1 Drug-likeness properties

Lipinski's Rule of Five (RO5)^[18], was used to evaluate the drug-likeness characteristics of the compounds. This evaluation was performed using pkCSM and ADMETLab 3.0.^[19,20] The RO5 assesses essential molecular properties significant for oral bioavailability, including molecular weight, octanol-water partition coefficient (logP), and hydrogen bond acceptors and donors.^[21] This criterion, a refinement of drug-likeness, aids in predicting whether a compound possesses the pharmacological or biological activity suitable for oral administration in humans.

2.4.2 ADMET Prediction

The evaluation of small molecules in medicinal chemistry and pharmacokinetics necessitates critical Absorption, Distribution, Metabolism, Excretion, and Toxicity (ADMET) studies.^[22] pkCSM and ADMETLab 3.0 were used to investigate the ADMET properties of possible therapeutic candidates. Key parameters such as caco2 permeability, human intestinal absorption, p-glycoprotein inhibition, cytochrome P450 enzymes inhibition, half-life ($t_{1/2}$), total clearance, acute oral toxicity, Ames toxicity, carcinogenicity,

hepatotoxicity, hematoxicity, nephrotoxicity, and human ether-a-go-go related gene (hERG) inhibition, were assessed.^[23-25] This was done by entering the Simplified Molecular Input Line Entry System (SMILES) of the ligands from PubChem into the webserver pkCSM and ADMETLab 3.0 respectively.

2.5 Molecular Docking

The study employed *in-silico* molecular docking techniques using AutoDock Vina and iGEMDock to evaluate the binding interactions of oxythiamine, phenylisocytosine and two analogues with the *plasmodium falciparum* transketolase enzyme (PDB ID: 8R3Q).

2.5.1 AutoDock Vina

AutoDock Vina was employed for structure-based virtual screening to predict ligand binding affinity to *Plasmodium falciparum* transketolase. Docking was performed with an exhaustiveness level of 8 to thoroughly explore conformational space.^[26] The grid box, defining the docking site, was positioned around the active pocket of the 8R3Q receptor, with dimensions of (44 × 44 × 44) for the X, Y, and Z axes, and a spacing of (1Å) centered on specific active pocket residues (Trp46, Ser47, Tyr48, Met50, Arg62, Asp63, His109, Thr111, Val114, Glu115, Tyr153, Asp160, Asn190, Ile194, Cys253, His266, Lys306, Asn310, Val427). The protein structure was optimized by adding polar hydrogen atoms and applying Gasteiger charges, then converted to PDBQT format.^[27,28] For each ligand, eight docking conformations were generated and scored using the London dG function, with the lowest-energy pose selected for further analysis.^[29,30]

2.5.2 iGEMDock

Molecular docking validation was conducted using iGEMDock version 2.1, which employed the “prepare binding site” feature to define docking parameters. A grid with an 8.0 Å radius centered on the active site was created. Precision parameters were set to ensure accuracy, including a population size of 800, 10 number of solutions, and 80.^[26,31] This setup enabled an exhaustive exploration of binding orientations and affinities, providing robust docking validation.

2.6 Molecular Mechanics (MM-GBSA)

MM-GBSA analysis was performed using the Prime MM-GBSA tool in Maestro version 12.5 to calculate relative binding free energies of each ligand. This method decomposes energy contributions (electrostatic interactions, van der Waals forces, hydrogen bonds, and solvation energies) to determine binding free energy.^[25,32] The binding free energy (ΔG_{bind}) was calculated as:

$$\Delta G_{\text{bind}} = \Delta E_{\text{MM}} + \Delta G_{\text{GB}} + \Delta G_{\text{SA}}$$

where ΔE_{MM} equals E_{ele} (electrostatic energy) + E_{vdw} (van der waals energy) + E_{Hbond} (hydrogen bond energy) + E_{int} (torsional angle energy) and represents molecular mechanical energy, ΔG_{GB} is the polar solvation energy, and ΔG_{SA} is the nonpolar solvation energy. The results from this analysis offered insights into the binding stability of each ligand. [33,34]

2.7 Molecular Dynamic (MD) Simulation

MD simulations were performed to evaluate the structural binding stability, conformational dynamics, and interaction modes of the protein-ligand complexes. [35] These simulations provide a powerful approach for examining atomic-level changes within the complexes under dynamic conditions. [26] The simulations were carried out using GROMACS software version 2022, which is widely recognized for its accuracy in simulating proteins, lipids, and nucleic acids. To initiate the simulations, the topologies of the protein and ligands were generated using CHARMM36 force fields and refined following protocols provided by GROMACS and CgenFF. [29] The protein-ligand complex was placed within a dodecahedron box filled with counterions and simple point charge (SPC) water molecules, using the 'genion' tool to create a neutralized, solvated environment suitable for simulation. [30]

To ensure system stability, an iterative energy minimization was conducted until the maximum force was reduced to less than 100 kJ/mol/nm, utilizing optimization algorithms like the steepest descent and conjugate gradient methods. [32] Once a stable conformation was established at 5000 steps with the steepest descent approach, the system underwent equilibration using the Verlet algorithm, from 0 to 300 K, over a period of 100 picoseconds (ps) with a time step of 2 femtoseconds (fs) for the NVT ensemble (constant Number of particles, Volume, and Temperature). This was followed by further equilibration using the Berendsen algorithm with a 2fs time step for 100 ps under the NPT ensemble (constant Number of particles, Pressure, and Temperature). The MD simulations were then conducted for a 50-nanosecond (ns) production run of the protein-ligand complexes. [29,30]

Post-simulation analysis was performed using Xmgrace, focusing on key parameters such as Root Mean Square Deviation (RMSD), Root Mean Square Fluctuation (RMSF), Radius of Gyration (ROG), and Intermolecular Hydrogen Bonds. [26,29-30] These analyses provided valuable insights into the stability and dynamic behavior of the protein-ligand complexes, allowing for a comprehensive understanding of their interaction mechanisms and stability under physiological conditions.

3.0 RESULTS AND DISCUSSION

3.1 PHYSICOCHEMICAL, PHARMACOKINETIC AND TOXICOLOGICAL PROFILING.

3.1.1 Drug likeness Prediction

The drug-likeness of phenylisocytosine, thioxopyrimidinone, and pyrimidinedione was assessed against Lipinski's Rule of Five (RO5) criteria, which are essential for predicting oral bioavailability in potential drug candidates. According to RO5, an ideal drug candidate should have a molecular weight <500 Da, <5 hydrogen bond donors, <10 hydrogen bond acceptors, and a log P <5, balancing hydrophilicity and lipophilicity to support efficient absorption and distribution.^[18,20] Table 1 summarizes the properties of each compound, including oxythiamine as a reference drug.

Table 1: Drug-likeness (Rule of 5) evaluation and physicochemical properties of oxythiamine (Reference drug), phenylisocytosine, thioxopyrimidinone, and pyrimidinedione.

Ligands	Molecular weight	H-bond donor	H-bond acceptor	Log p	Inference
Compound Identifier	< 500	< 5	< 10	< 5	MEET R05
Oxythiamine (reference Drug)	266.1	2	5	-0.977	Accepted
2-amino-6-phenylpyrimidin-4(1H)-one (Phenylisocytosine)	189.09	3	4	0.921	Accepted
6-Phenylpyrimidine-2,4(1H,3H)-dione (thioxopyrimidinone)	190.07	2	4	1.083	Accepted
6-Phenyl-2-thioxo-2,3-dihydropyrimidine-4(1H)-one (pyrimidinedione)	206.05	2	3	1.489	Accepted

All tested compounds met RO5 requirements, indicating their potential as orally active agents. Oxythiamine, with a molecular weight of 266.1 Da, 2 hydrogen bond donors, 5 acceptors, and a log P of -0.977, was within RO5 limits, yet its high hydrophilicity (negative log P) could hinder membrane permeability, impacting bioavailability unless aided by active transport.^[36] Phenylisocytosine displayed ideal drug-likeness characteristics with a molecular weight of 189.09 Da, 3 hydrogen bond donors, 4 acceptors, and a log P of 0.921, suggesting a favorable hydrophilicity-lipophilicity balance that could facilitate effective membrane permeability and oral bioavailability.

Thioxopyrimidinone and pyrimidinedione, with molecular weights of 190.07 Da and 206.05 Da, respectively, also adhered to RO5, exhibiting 2 hydrogen bond donors and acceptable acceptor values. Their log P values, 1.083 for thioxopyrimidinone and 1.489 for pyrimidinedione, suggest better lipophilicity compared to phenylisocytosine, which could enhance absorption through lipid membranes. However,

increased lipophilicity also raises bioaccumulation risks, potentially causing toxicity with prolonged use.^[37]Therefore, although favorable, careful monitoring is essential to ensure safe pharmacokinetic profiles.

3.1.2 ADMET Evaluation

ADMET properties—Absorption, Distribution, Metabolism, Excretion, and Toxicity—of the ligands were evaluated using pkCSM and ADMETLab 3.0 to assess clinical efficacy and safety.^[20]All compounds demonstrated excellent Caco-2 permeability and high human intestinal absorption, supporting their likelihood for effective oral bioavailability. However, oxythiamine displayed poor Caco-2 permeability and limited human intestinal absorption, indicating potential issues with passive absorption that may limit clinical efficacy.^[38]Notably, all ligands inhibited P-glycoprotein, which could reduce drug efflux, though oxythiamine's poor permeability remains a challenge. In terms of metabolism, all ligands were non-inhibitors of CYP450 enzymes such as CYP2D6 and CYP3A4, reducing the risk of drug-drug interactions, a significant factor for potential co-therapies. Oxythiamine, however, moderately inhibited CYP1A2, suggesting a risk of interactions when co-administered with drugs metabolized by this enzyme. The absence of CYP inhibition in phenylisocytosine and its analogs indicates a favorable metabolic profile, further supporting their potential safety in combination therapies. Regarding excretion, all compounds demonstrated excellent clearance rates, aside from oxythiamine, which had poor clearance and a prolonged half-life, increasing the risk of toxicity from accumulation.^[39]Conversely, the other ligands' effective clearance suggests reduced toxicity risks, enabling safe excretion.

Toxicity profiles highlighted that none of the ligands were associated with hERG inhibition, mitigating cardiotoxicity risks. While oxythiamine showed nephrotoxicity, posing a risk for kidney damage, phenylisocytosine, thioxopyrimidinone, and pyrimidinedione were non-toxic in terms of hepatotoxicity and hematotoxicity, indicating their suitability as safer agents. Additionally, oxythiamine exhibited a higher risk of carcinogenicity compared to the other ligands, suggesting a limited therapeutic window. The moderate AMES toxicity and carcinogenicity of the other ligands warrant monitoring but do not preclude further investigation as potential antimalarial drugs.^[40,41]

Table2: ADMET properties of oxythiamine, phenylisocytosine, thioxopyrimidinone, and pyrimidinedione (Reference drug).

Ligands	Absorption and Distribution	Metabolism	Excretion and Toxicity
---------	-----------------------------	------------	------------------------

Compound Identifier	Caco2 Permeability	Human Intestinal absorption	P-glycoprotein Inhibitor	CYP2D6	CYP3A4	CYP1A2	CYP2C19	CYP2C9	Half-life	Total Clearance	Nephrotoxicity	Acute oral toxicity	AMES toxicity	Carcinogenicity	HERG inhibitor	Hepatotoxicity	Hematotoxicity
Oxythiamine (Reference Drug)	R	R	G	G	G	B	G	G	0.894	B	R	R	G	R	G	G	G
Phenylisocytosine	G	G	G	G	G	G	G	G	1.17	G	G	R	B	B	G	G	G
Thioxopyrimidinone	G	G	G	G	G	G	G	G	1.091	G	G	R	B	B	G	G	G
Pyrimidinedione	G	G	G	G	G	G	G	G	1.074	G	G	R	B	B	G	G	G

G = Excellent B = Medium R = Poor

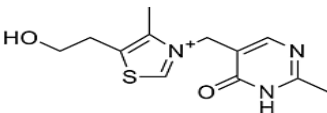
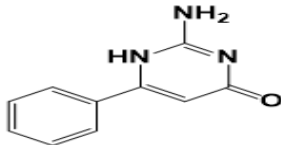
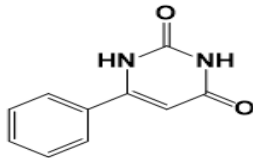
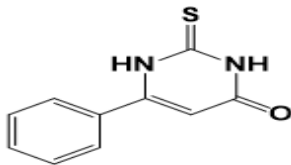
3.2 MOLECULAR DOCKING

Molecular docking analyses offered critical insights into the binding interactions of phenylisocytosine, thioxopyrimidinone, and pyrimidinedione with *Plasmodium falciparum* transketolase, in comparison to oxythiamine. Strong binding affinities are associated with effective inhibition, as stable interactions within the enzyme's active site are crucial for halting catalytic activity. Oxythiamine demonstrated weaker binding affinities, with scores of -5.2 kcal/mol (AutoDock Vina) and -7.1 kcal/mol (iGEMDock). While oxythiamine formed hydrogen bonds with residues such as Met50, Asp63, and Asn310, additional interactions involving Ser47, Tyr153, and Lys306 contributed to its binding. However, the lower binding energies suggest that oxythiamine may be a less effective inhibitor relative to other ligands, with weaker binding potentially reducing inhibitory potency.

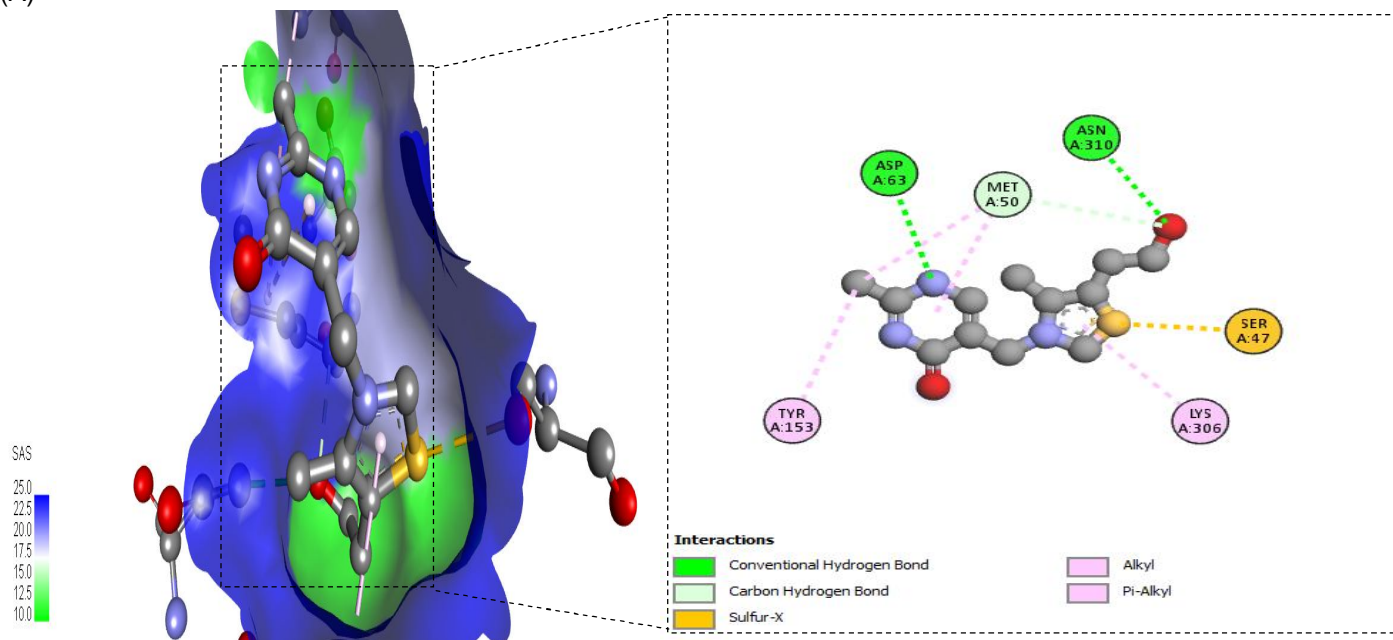
Phenylisocytosine showed the highest binding affinity, scoring -6.3 kcal/mol in AutoDock Vina and -8.5 kcal/mol in iGEMDock. This strong affinity was due to multiple hydrogen bonds with active site residues, including Trp46, Ser47, and Asn310, as well as interactions with Tyr48 and Lys306, which stabilized the phenylisocytosine-transketolase complex. Such strong binding interactions support phenylisocytosine's potential as an effective inhibitor of transketolase. Thioxopyrimidinone demonstrated a high binding affinity, scoring -6.2 kcal/mol (AutoDock Vina) and -8.5 kcal/mol (iGEMDock), with hydrogen bonds to Asp160, Asn190, Cys253, and His266, and additional hydrophobic interactions with Ile194. The extensive hydrogen bonding and hydrophobic contacts suggest stable binding, supporting thioxopyrimidinone's efficacy as an antimalarial agent. Pyrimidinedione also exhibited favorable binding, with scores of -6.2 kcal/mol (AutoDock Vina) and -8.3 kcal/mol (iGEMDock), forming hydrogen bonds with residues Arg62, Glu115, Val114, and Ala427, as well as hydrophobic interactions with His109 and Thr111. This binding

pattern contributes to stable ligand anchoring in the active site, supporting pyrimidinedione's inhibitory potential. The comparative analysis of docking results (Table 3, Figure 2 and 3) highlights the superior binding affinities and interaction profiles of phenylisocytosine, thioxopyrimidinone, and pyrimidinedione over oxythiamine. Stronger binding interactions indicate their potential as effective inhibitors of *Plasmodium falciparum* transketolase, aligning with previous studies that emphasize stable binding as a determinant of inhibitor efficacy.^[42]

Table 3: provides information about the three ligands and a reference drug, presenting data on each ligand name, binding affinities, number of hydrogen bond interactions, other interactions and 2D structures. The three ligands showed higher binding affinity compared to oxythiamine, indicating their potential effectiveness for the treatment of malaria parasites infection.

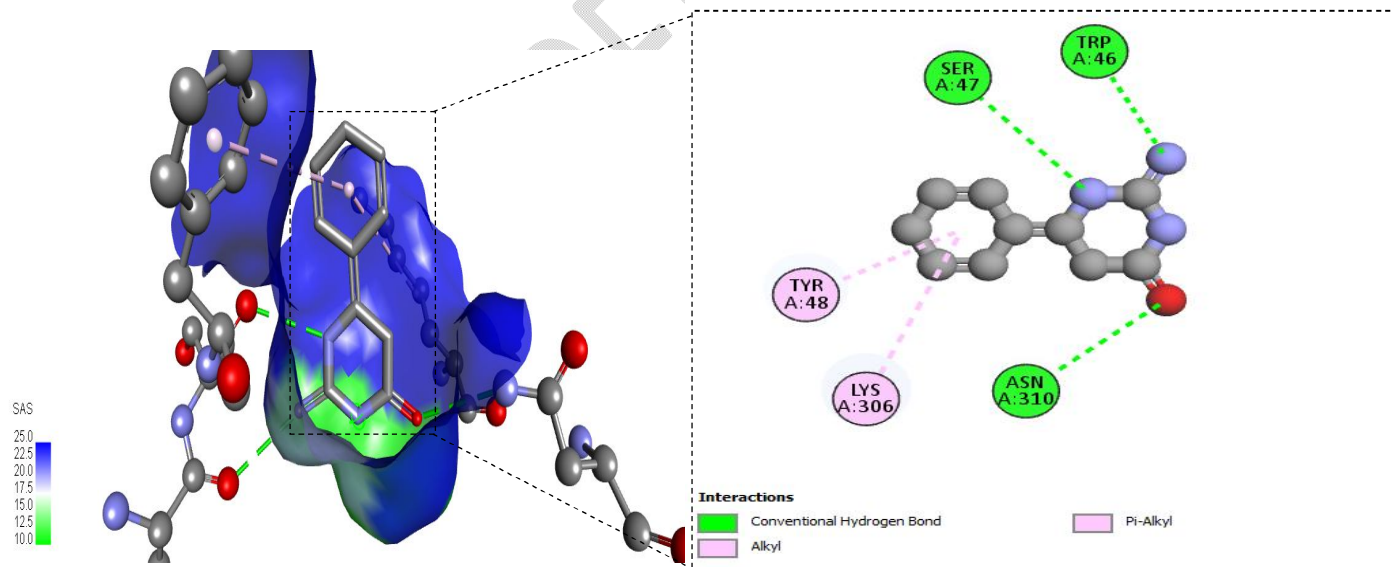
Ligands	Binding Energy (AutoDock Vina) Kcal/mol)	Binding Energy (iGEMDock) Kcal/mol)	H-bond Interaction	Other Interaction	2-D structure
Oxythiamin (Reference Drug)	-5.2	-7.1	Met50, Asp63, Asn310	Ser47, Tyr153, Lys306	
Phenylisocytosine	-6.3	-8.5	Trp46, Ser47, Asn310	Tyr48, Lys306	
Thioxopyrimidinone	-6.2	-8.5	Asp160, Asn190, Cys253, His266	Ile194	
Pyrimidinedione	-6.2	-8.3	Arg62, Glu115, Val114, Ala427	His109, Thr111	

(A)



8R3Q_OXYTHIAMINE

(B)



8R3Q_PHENYLISOCYTOSINE

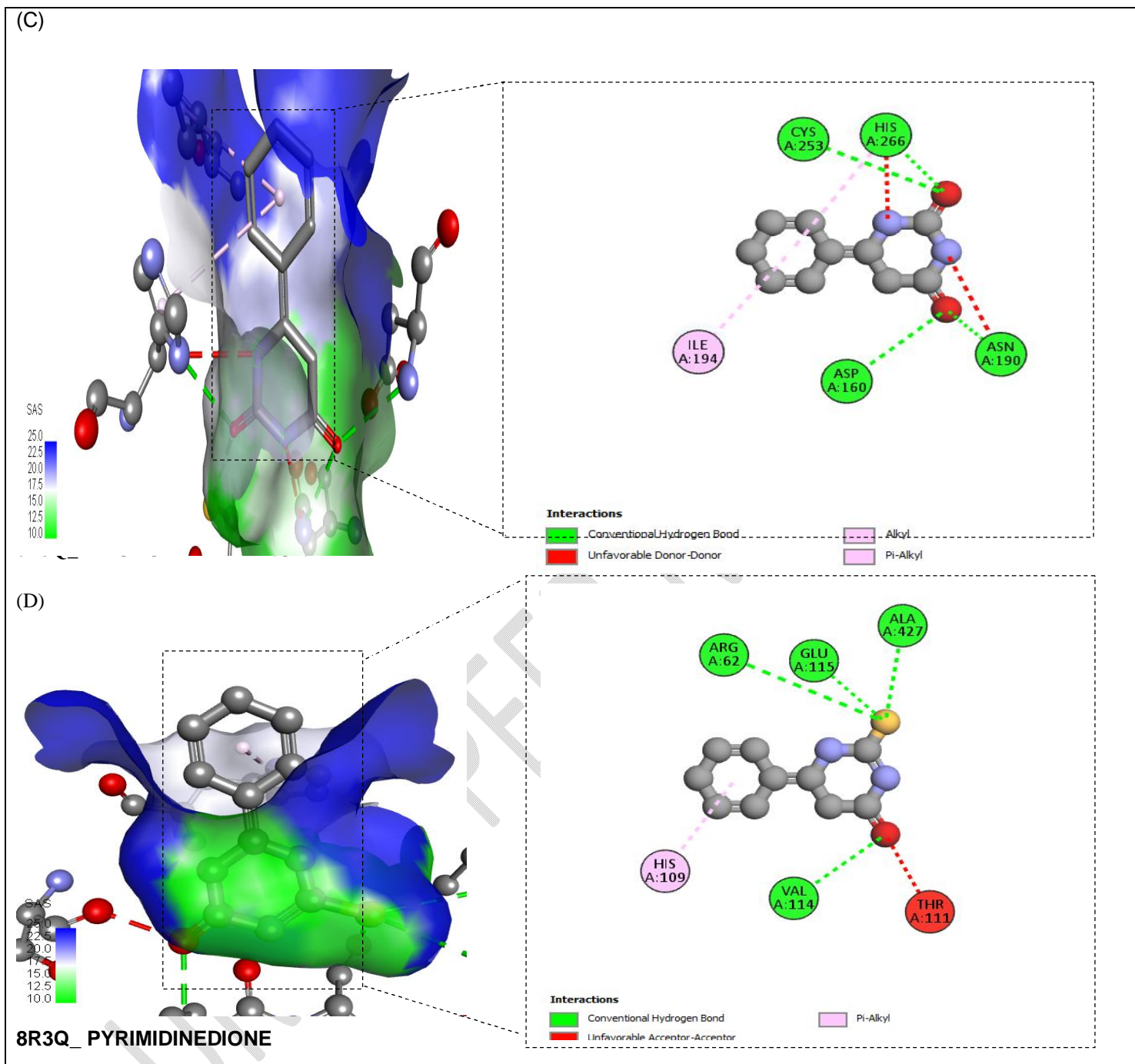


Figure 2. Molecular interaction between the three ligands and the reference drug at the active site of *plasmodium falciparum* transketolase (8R3Q) (A) Oxythiamine (reference drug) (b) Phenylisocytosine (c) Thioxopyrimidinone(d) Pyrimidinedione. The structures were rendered using Biovia Discovery Studio 2021.

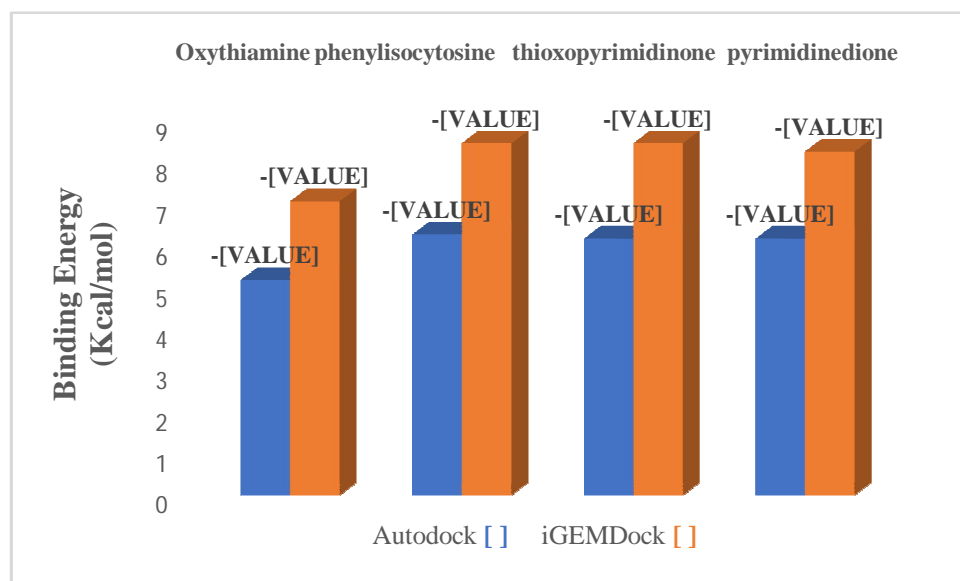


Figure 3: Binding affinities of the three ligands and the reference drug in Auto-dock vina and IGEM Dock.

3.3 MOLECULAR MECHANICS-GENERALIZED BORN SURFACE AREA (MM-GBSA)

MM-GBSA analysis was conducted to provide insights into the binding energies and stability of the ligand-protein complexes, with the results summarized in Table 4 and Figure 4. The MM-GBSA approach enabled a breakdown of binding free energy into key components, including van der Waals forces, hydrogen bonding, covalent bonding, and polar solvation. Understanding these energy components is essential for interpreting ligand-protein interactions and stability within the complexes.

Table 4: MM-GBSA binding free energies of Oxythiamine, Phenylisocytosine, Thioxopyrimidinone, and Pyrimidinedione.

Ligands	MMGBSA ΔG Bind H-bond (Kcal/mol)	MMGBSA ΔG Bind Covalent bond (Kcal/mol)	MMGBSA ΔG Bind Vander Waal Forces (Kcal/mol)	MMGBSA ΔG Bind Polar Solvation (Kcal/mol)	MMGBSA ΔG Overall Binding energy (Kcal/mol)
Oxythiamine	-3.12	2.75	-33.6	30.91	-16.85
Phenylisocytosine	-3.16	2.91	-24.22	45.45	-26.05
Thioxopyrimidinone	-3.34	4.49	-20.65	19.3	-25.48
Pyrimidinedione	-3.38	2.5	-20.95	-4.95	-24.44

Van der Waals interactions emerged as a significant contributor to binding stability across all ligands. Oxythiamine demonstrated the strongest van der Waals interaction (-33.6 kcal/mol), enhancing its binding affinity; however, its overall binding energy was limited to -16.85 kcal/mol due to high polar solvation energy (30.91 kcal/mol). This high solvation energy indicates substantial desolvation costs, which counter the binding stability provided by van der Waals forces, thus weakening oxythiamine's stability as a ligand. In contrast, phenylisocytosine exhibited a balanced combination of interactions, achieving the lowest overall binding energy (-26.05 kcal/mol), making it the most stable ligand. Despite a high desolvation penalty (polar solvation energy of 45.45 kcal/mol), phenylisocytosine's favorable van der Waals interactions (-24.22 kcal/mol) and moderate hydrogen bonding (-3.16 kcal/mol) contributed to a strong binding with the target protein. This combination highlights phenylisocytosine's stability and suggests its potential as an effective inhibitor of *Plasmodium falciparum* transketolase. Thioxopyrimidinone showed comparable binding stability, with an overall binding energy of -25.48 kcal/mol, supported by strong hydrogen bonding (-3.34 kcal/mol) and moderate van der Waals interactions (-20.65 kcal/mol). Its lower polar solvation energy (19.3 kcal/mol) indicated a reduced desolvation cost, enhancing its binding stability. These factors indicate that thioxopyrimidinone forms a balanced and stable interaction with the enzyme. Pyrimidinedione, while showing promising van der Waals interactions (-20.95 kcal/mol), had a slightly weaker binding energy (-24.44 kcal/mol), largely due to its polar solvation energy (-4.95 kcal/mol). Despite forming stable hydrogen bonds (-3.38 kcal/mol), pyrimidinedione's binding stability was slightly lower than that of phenylisocytosine and thioxopyrimidinone, making it a somewhat less stable ligand.

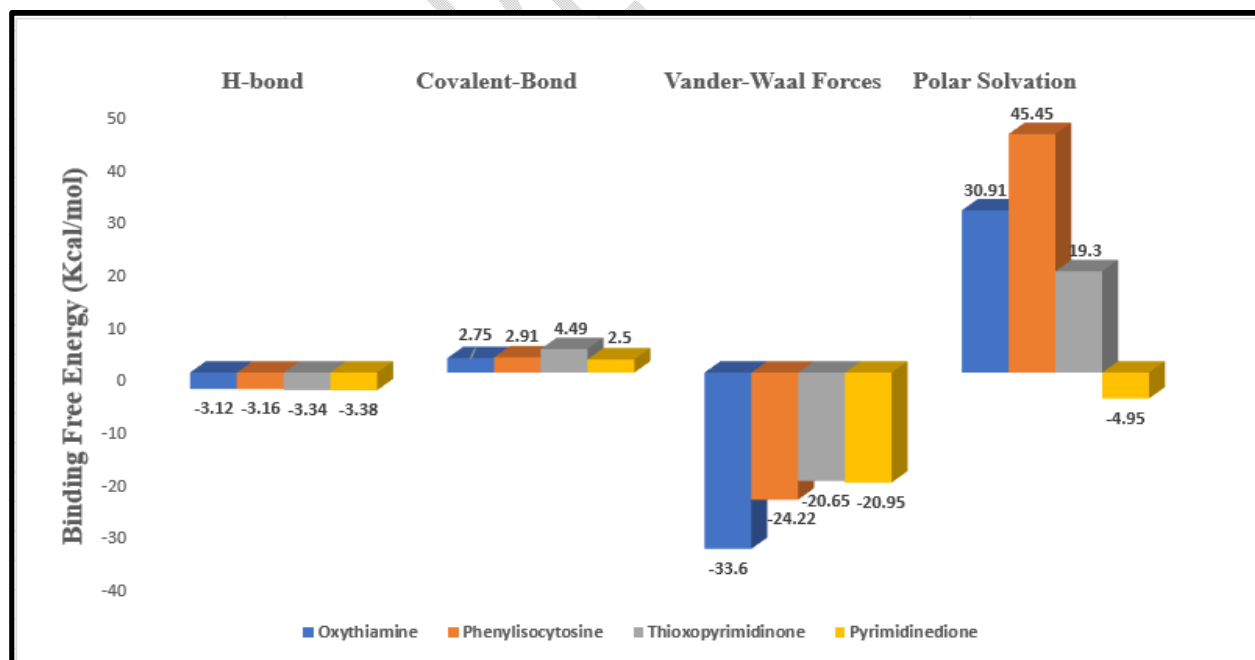


Figure 4: MMGBSAΔG Bind H-bond, Covalent bond, Vander waal forces, and Polar solvation of

Phenylisocytosine, Thioxopyrimidinone, Pyrimidinedione, and the reference drug (oxythiamine) in Maestro 12.5

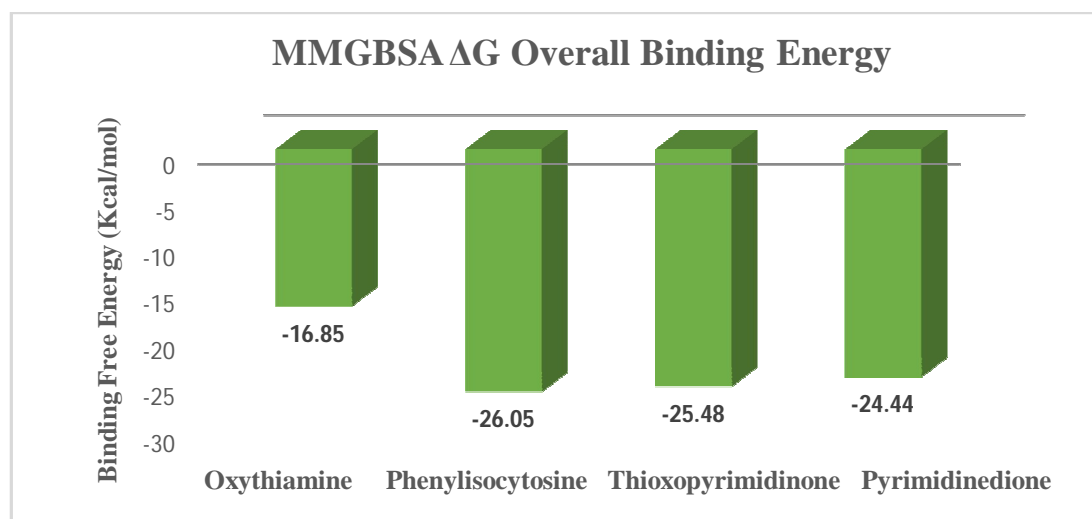


Figure 5:MMGBSA ΔG overall binding energy for Phenylisocytosine, Thioxopyrimidinone, Pyrimidinedione, and the reference drug (oxythiamine) in Maestro 12.5.

3.4 SELECTION OF LEAD COMPOUNDS FOR MD SIMULATION.

After an initial filtering process through structure-based virtual screening (molecular docking and molecular mechanics) and ligand-based virtual screening, including Lipinski's rule of five and ADMET evaluation, 2-amino-6-phenylpyrimidin-4(1H)-one (Phenylisocytosine) and 6-Phenylpyrimidine-2,4(1H,3H)-dione (Thioxopyrimidinone) were selected for MD simulations alongside the reference drug, Oxythiamine. These two ligands exhibited favourable pharmacokinetic profiles, meeting drug-likeness criteria while demonstrating strong binding affinities in molecular docking studies. In particular, their ability to engage in stable interactions with the target protein and their promising ADMET properties made them viable candidates for further molecular dynamic simulation.

3.5 MOLECULAR DYNAMICS (MD)

MD simulations assessed the stability, flexibility, and interaction strength of the protein-ligand complexes over time, analyzing key parameters such as RMSD, RMSF, ROG, and H-bond (Table 5). These metrics provide insights into the complexes' behavior under physiological conditions

Table 5: Average values of RMSD, RMSF, ROG, and H-bond of all simulated complexes.

Compound Identifier	Average RMSD values (nm)	Average RMSF values (nm)	Average H-bond values (nm)	Average ROG values (nm)
Oxythiamine	0.474347	0.138127	0.08173	3.022909

2-amino-6-phenylpyrimidin-4(1H)-one (Phenylisocytosine)	0.303705	0.122734	1.023494	3.013614
6-Phenylpyrimidine-2,4(1H,3H)-dione (Thioxopyrimidinone)	0.327217	0.131814	0.422394	2.99662

3.5.1 RMSD

RMSD values reflect the overall stability of the protein-ligand complex by measuring the deviation in atomic positions over time. Oxythiamine displayed the highest RMSD value (0.474 nm), which suggests that it undergoes significant conformational changes during the simulation. This high value indicates that oxythiamine forms a less stable complex, likely resulting from weaker interactions with the protein, leading to greater flexibility and movement away from the initial binding site. In contrast, phenylisocytosine exhibited the lowest RMSD value (0.303 nm), reflecting a highly stable complex with minimal deviation from its initial conformation. This lower RMSD suggests that phenylisocytosine maintains a strong and consistent interaction with the target protein throughout the simulation, reinforcing its potential as an effective inhibitor. Thioxopyrimidinone showed a slightly higher RMSD value (0.327 nm) than phenylisocytosine, but it still demonstrated good stability. These results highlight that phenylisocytosine forms the most stable complex, followed by Thioxopyrimidinone, while oxythiamine exhibited the least stable interactions.

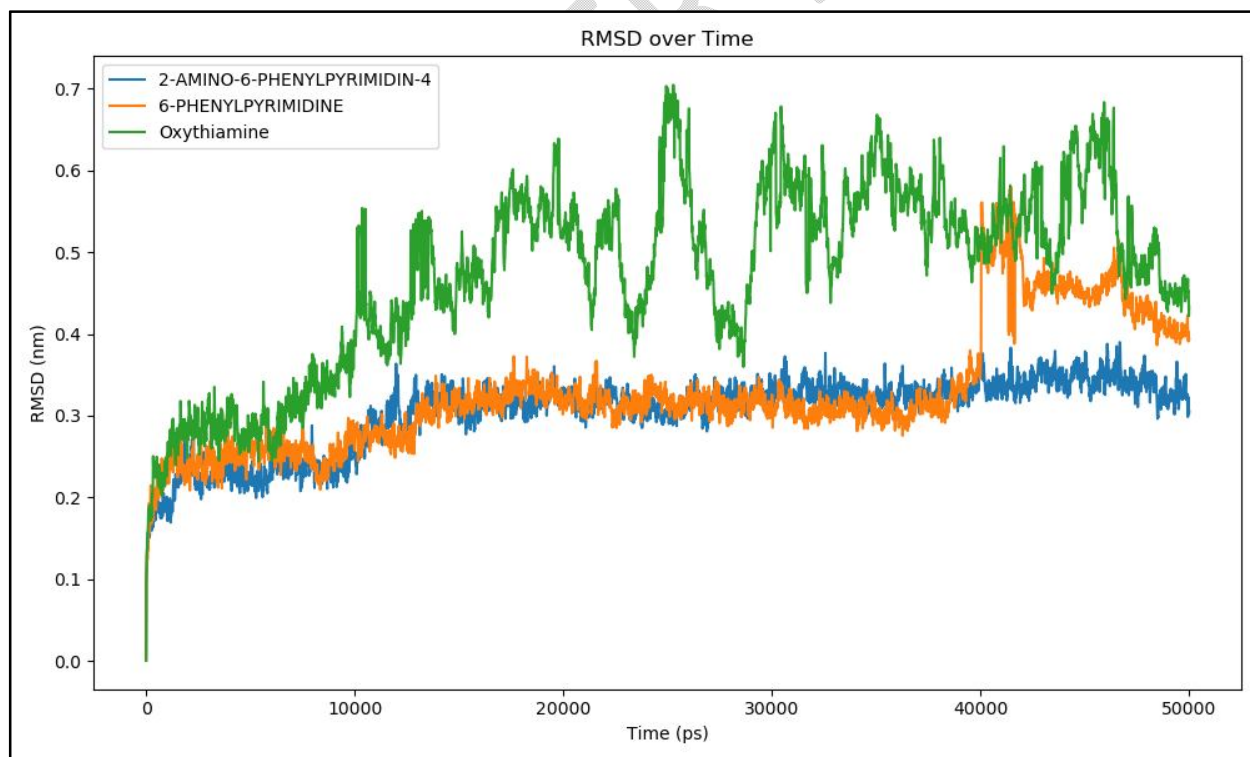


Figure6: RMSD Plot Showing the Stability of 2-Amino-6-Phenylpyrimidin-4 (Phenylisocytosine), 6-Phenylpyrimidine(Thioxopyrimidinone), and Oxythiamine Over 50 ns of Molecular Dynamics Simulation.

3.5.2 RMSF

RMSF values provide insight into the flexibility of individual residues within the protein-ligand complex. Phenylisocytosine once again exhibited superior performance with the lowest RMSF value (0.122 nm), indicating minimal fluctuations and strong interactions with specific protein residues. This suggests that the binding region remains stable when interacting with phenylisocytosine, further supporting its potential as a potent inhibitor. Thioxopyrimidinone exhibited an RMSF value of 0.131 nm, indicating slightly more flexibility than phenylisocytosine but still maintaining a stable interaction. Oxythiamine, with the highest RMSF value (0.138 nm), showed greater residue flexibility, suggesting weaker binding and a less stable complex. These findings reinforce the conclusion that phenylisocytosine forms the most rigid and stable interactions with the protein, while oxythiamine exhibits greater flexibility and weaker binding, which could undermine its inhibitory effectiveness.

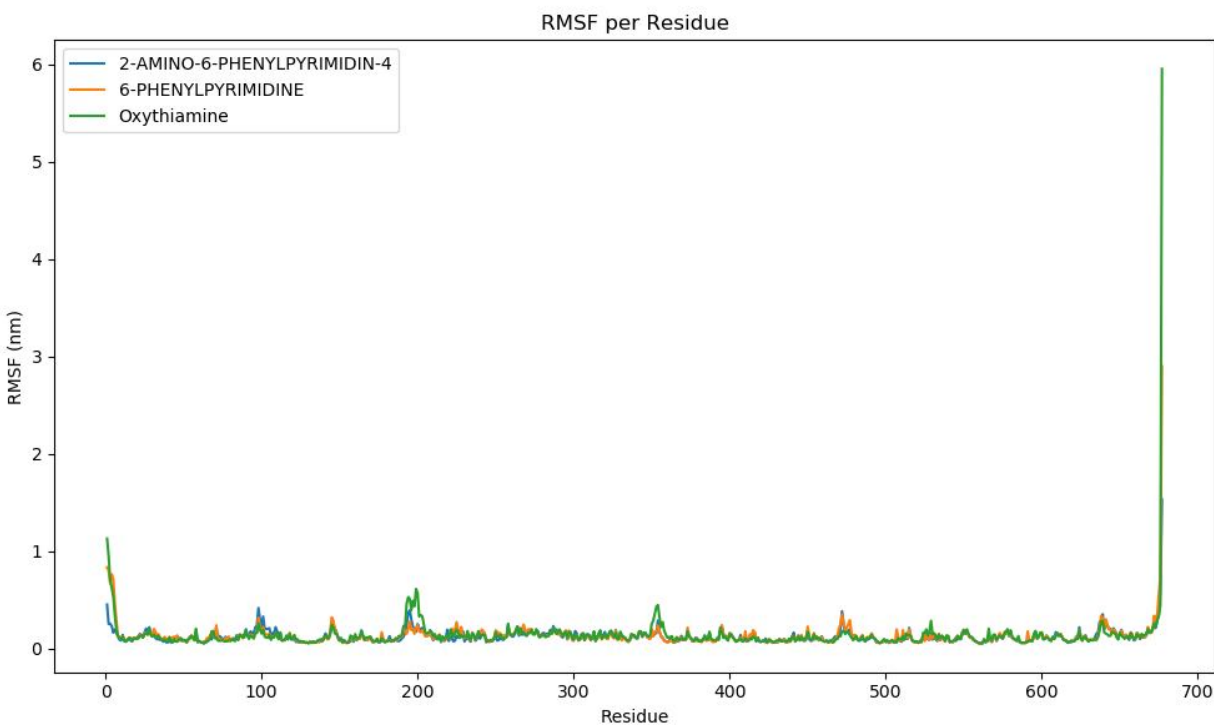


Figure7: RMSF Plot Showing the Stability of 2-Amino-6-Phenylpyrimidin-4 (Phenylisocytosine), 6-Phenylpyrimidine (Thioxopyrimidinone), and Oxythiamine Over 50 ns of Molecular Dynamics Simulation.

3.5.3 ROG

ROG is a measure of the compactness of the protein-ligand complex, with lower values indicating a more tightly packed and stable structure. Oxythiamine exhibited the highest ROG value (3.022 nm), indicating a less compact and more expanded structure. This suggests that the complex involving oxythiamine is not as tightly bound, resulting in weaker interactions and a less stable binding profile. Phenylisocytosine, with

an ROG value of 3.013 nm, formed a more compact and stable complex, further confirming its strong interaction with the enzyme's active site. Thioxopyrimidinone demonstrated the lowest ROG value (2.996 nm), indicating that it forms the most compact complex among the tested ligands. This compactness is a positive indicator of stable binding, as the ligand remains tightly seated within the binding pocket, leading to greater stability. The ROG results align with the RMSD and hydrogen bonding data, suggesting that both phenylisocytosine and Thioxopyrimidinone form more stable and tightly packed complexes compared to oxythiamine, which showed the least favorable compactness.

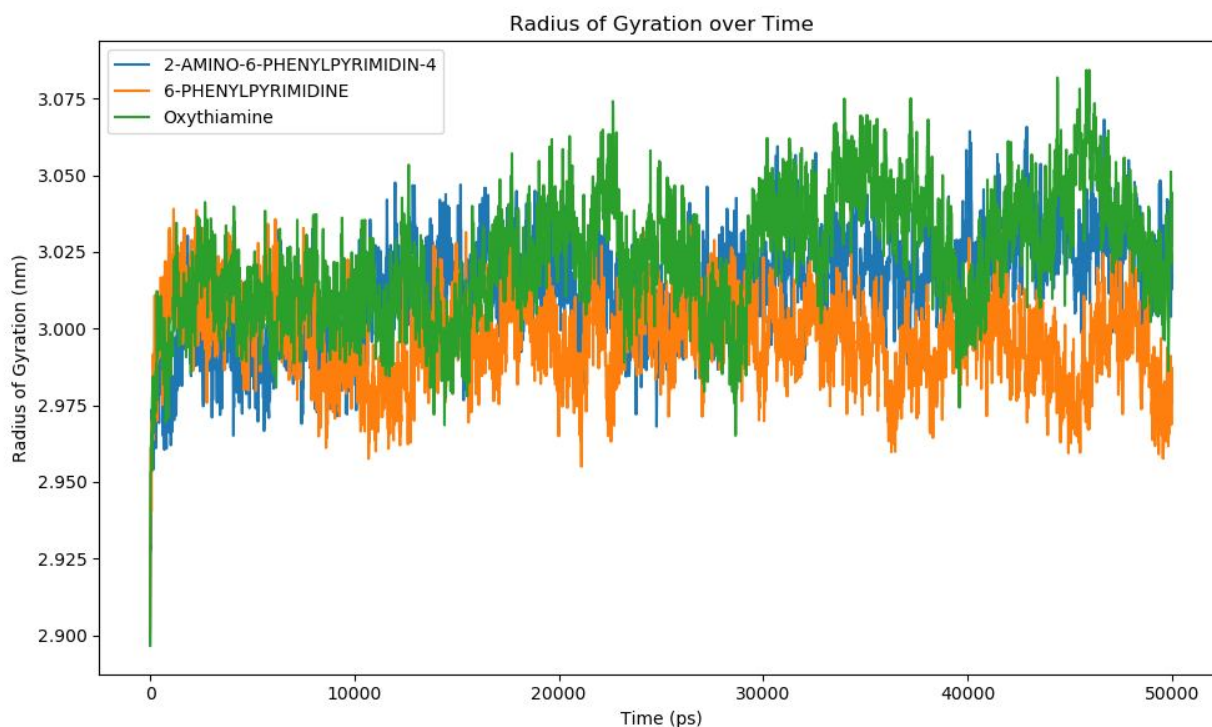


Figure 8: RoG Plot Showing the Stability of 2-Amino-6-Phenylpyrimidin-4 (Phenylisocytosine), 6-Phenylpyrimidine (Thioxopyrimidinone), and Oxythiamine Over 50 ns of Molecular Dynamics Simulation.

3.5.4 H-bonding

Hydrogen bonding is crucial for stabilizing protein-ligand interactions, and the number of hydrogen bonds formed during the MD simulation directly correlates with interaction strength. Phenylisocytosine formed an average of 1.023 hydrogen bonds, indicating strong and stable interactions with the target protein. This relatively high number of hydrogen bonds supports the hypothesis that phenylisocytosine establishes robust and stable interactions, contributing to the overall stability of the complex. Thioxopyrimidinone formed 0.422 hydrogen bonds on average, which, although lower than phenylisocytosine, still suggests a relatively stable interaction. In contrast, oxythiamine formed only 0.081 hydrogen bonds, reflecting much weaker interactions and reduced stability. The limited hydrogen bonding capability of oxythiamine

suggests that it does not effectively stabilize the protein-ligand complex, likely contributing to its poorer performance in maintaining binding stability.

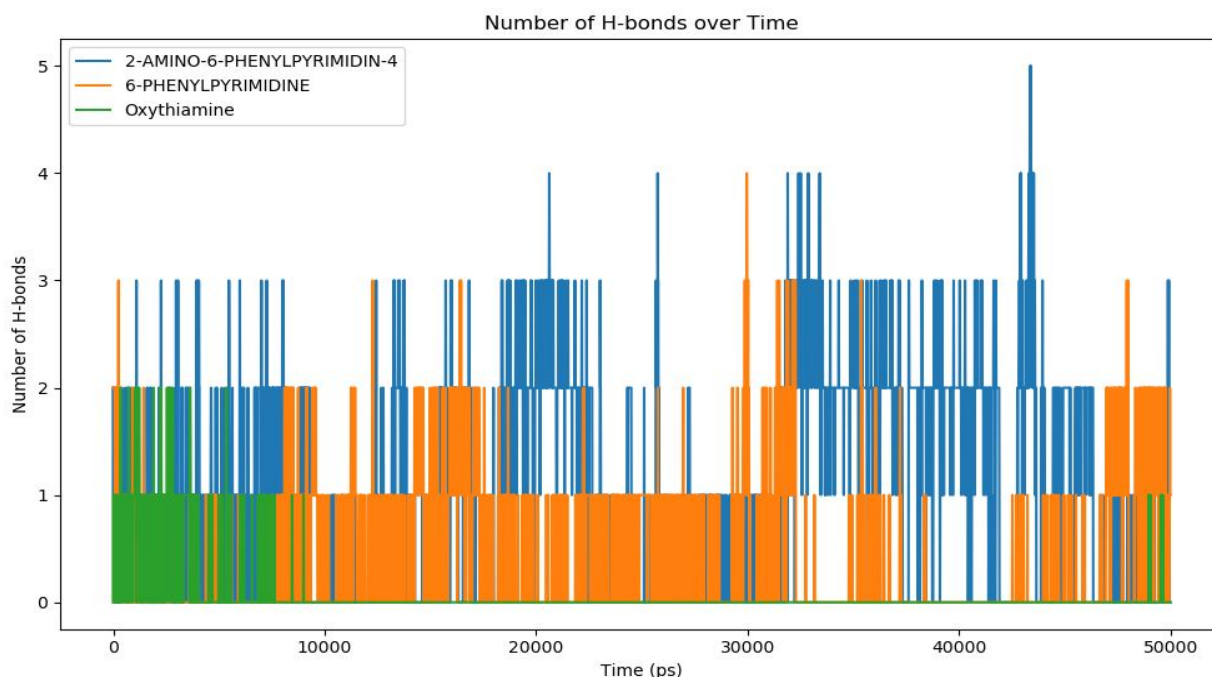


Figure 9: H-bonding Plot Showing the Stability of 2-Amino-6-Phenylpyrimidin-4 (Phenylisocytosine), 6-Phenylpyrimidine (Thioxopyrimidinone), and Oxythiamine Over 50 ns of Molecular Dynamics Simulation.

4.0 CONCLUSION

This study investigated the potential of phenylisocytosine and its analogs, thioxopyrimidinone and pyrimidinedione, as inhibitors of *Plasmodium falciparum* transketolase, a key enzyme in the pentose phosphate pathway, to address drug-resistant malaria. Through comprehensive *in silico* approaches—including pharmacokinetic evaluation, molecular docking, molecular mechanics, and molecular dynamics simulations—phenylisocytosine emerged as the most promising candidate, demonstrating favorable drug-likeness, safety profiles, superior binding affinity, stability, and strong interaction with the target protein. In comparison, the reference drug, oxythiamine, showed poor pharmacokinetics, weaker binding, and reduced stability. Given its favorable computational profile, phenylisocytosine warrants further investigation, with synthesis and experimental validation through *in vitro* and *in vivo* assays essential to confirm its efficacy against *Plasmodium falciparum*. These findings underscore the importance of targeting alternative metabolic pathways in *Plasmodium falciparum* and lay the groundwork for developing phenylisocytosine as a novel antimalarial agent.

GLOSSARY

Abbreviation

Meaning

2D Two-Dimensional

3D Three-Dimensional

ACTs Artemisinin-based Combination Therapies

ADMET Absorption, Distribution, Metabolism, Excretion, and Toxicity

CASTp Computed Atlas of Surface Topography of Proteins

CGENFF CHARMM General Force Field

CYP Cytochrome P450 (e.g., CYP1A2, CYP2C19, CYP2C9, CYP2D6, CYP3A4)

hERG Human Ether-à-go-go Related Gene

LBDD Ligand-Based Drug Design

MD Molecular Dynamics

MM-GBSA Molecular Mechanics Generalized Born Surface Area

NPT Constant Number of particles, Pressure, and Temperature (ensemble)

NVT Constant Number of particles, Volume, and Temperature (ensemble)

PDB Protein Data Bank

PPP Pentose Phosphate Pathway

RMSD Root Mean Square Deviation

RMSF Root Mean Square Fluctuation

RO5 Rule of Five

ROG Radius of Gyration

SPC Simple Point Charge (water model used in simulations)

SBDD Structure-Based Drug Design

DECLARATION OF GENERATIVE AI AND AI-ASSISTED TECHNOLOGIES IN THE WRITING PROCESS

During the preparation of this work, the authors used OpenAI's ChatGPT and QuillBot paraphrasing tool in order to enhance clarity, improve language precision, and streamline complex ideas. These tools were instrumental in refining the manuscript's readability and conciseness, ensuring that technical details were clearly communicated. After using this tool, the authors reviewed and edited the content as needed and takes full responsibility for the content of the publication.

REFERENCES

1. Okombo, J., & Chibale, K. (2018). Recent updates in the discovery and development of novel antimalarial drug candidates. *MedChemComm*, 9(3), 437-453. <https://doi.org/10.1039/C7MD00637C>
2. Amelo, W., & Makonnen, E. (2021). Efforts Made to Eliminate Drug-Resistant Malaria and Its Challenges. *BioMed Research International*, 2021(1), 5539544. <https://doi.org/10.1155/2021/5539544>
3. World malaria report. (2023). Geneva: World Health Organization; 2023. Licence: CC BY-NC-SA 3.0 IGO. ISBN 978-92-4-008617-3. <https://apps.who.int/iris>
4. Shibeshi, M. A., Kifle, Z. D., & Atnafie, S. A. (2020). Antimalarial drug resistance and novel targets for antimalarial drug discovery. *Infection and drug resistance*, 4047-4060. <http://doi.org/10.2147/IDR.S279433>
5. Hanboonkunupakarn, B., Tarning, J., Pukrittayakamee, S., & Chotivanich, K. (2022). Artemisinin resistance and malaria elimination: Where are we now?. *Frontiers in Pharmacology*, 13, 876282. <https://doi.org/10.3389/fphar.2022.876282>
6. Ginsburg, H. (2016). The biochemistry of Plasmodium falciparum: An updated overview. *Advances in Malaria Research*, 219-290. <https://doi.org/10.1002/9781118493816.ch9>
7. Kumar, S., Bhardwaj, T. R., Prasad, D. N., & Singh, R. K. (2018). Drug targets for resistant malaria: historic to future perspectives. *Biomedicine & Pharmacotherapy*, 104, 8-27. <https://doi.org/10.1016/j.biopha.2018.05.009>
8. Boateng, R. A., Tasthan Bishop, Ö., & Musyoka, T. M. (2020). Characterisation of plasmodial transketolases and identification of potential inhibitors: An *in silico* study. *Malaria journal*, 19, 1-19. <https://doi.org/10.1186/s12936-020-03512-1>

9. Bhunia, S. S., Saxena, M., & Saxena, A. K. (2021). Ligand-and structure-based virtual screening in drug discovery. In *Biophysical and Computational Tools in Drug Discovery* (pp. 281-339). Cham: Springer International Publishing. https://doi.org/10.1007/7355_2021_130
10. Tiwari, A., & Singh, S. (2022). Computational approaches in drug designing. In *Bioinformatics* (pp. 207-217). Academic Press. <https://doi.org/10.1016/B978-0-323-89775-4.00010-9>
11. Fu, Y., Zhao, J., & Chen, Z. (2018). Insights into the molecular mechanisms of protein-ligand interactions by molecular docking and molecular dynamics simulation: a case of oligopeptide binding protein. *Computational and mathematical methods in medicine*, 2018(1), 3502514. <https://doi.org/10.1155/2018/3502514>
12. Abdel-Haleem, A. M. (2019). Comparative metabolic modeling and analysis of human pathogens. KAUST Research Repository. <https://doi.org/10.25781/KAUST-9G8OS>
13. Tian, W., Chen, C., Lei, X., Zhao, J., & Liang, J. (2018). CASTp 3.0: computed atlas of surface topography of proteins. *Nucleic acids research*, 46(W1), W363-W367. <https://doi.org/10.1093/nar/gky473>
14. O'Boyle, N. M., Banck, M., James, C. A., Morley, C., Vandermeersch, T., & Hutchison, G. R. (2011). Open Babel: An open chemical toolbox. *Journal of cheminformatics*, 3(1), 1-14. <https://doi.org/10.1186/1758-2946-3-33>
15. Huey, R., Morris, G. M., & Forli, S. (2012). Using AutoDock 4 and AutoDock vina with AutoDockTools: a tutorial. The Scripps Research Institute Molecular Graphics Laboratory, 10550(92037), 1000. <http://vina.scripps.edu>.
16. Hsu, K. C., Chen, Y. F., Lin, S. R., & Yang, J. M. (2011). iGEMDOCK: a graphical environment of enhancing GEMDOCK using pharmacological interactions and post-screening analysis. *BMC bioinformatics*, 12, 1-11. <https://doi.org/10.1186/1471-2105-12-S1-S33>
17. Scholz, C., Knorr, S., Hamacher, K., & Schmidt, B. (2015). DOCKTITE □ A Highly Versatile Step-by-Step Workflow for Covalent Docking and Virtual Screening in the Molecular Operating Environment. *Journal of chemical information and modeling*, 55(2), 398-406. <https://doi.org/10.1021/ci500681r>
18. Lipinski, C. A. (2004). Lead-and drug-like compounds: the rule-of-five revolution. *Drug discovery today: Technologies*, 1(4), 337-341. <https://doi.org/10.1016/j.ddtec.2004.11.007>
19. Pires, D. E., Blundell, T. L., & Ascher, D. B. (2015). pkCSM: predicting small-molecule pharmacokinetic and toxicity properties using graph-based signatures. *Journal of medicinal chemistry*, 58(9), 4066-4072. <https://doi.org/10.1021/acs.jmedchem.5b00104>
20. Fu, L., Shi, S., Yi, J., Wang, N., He, Y., Wu, Z., ... & Cao, D. (2024). ADMETlab 3.0: an updated comprehensive online ADMET prediction platform enhanced with broader coverage, improved performance, API functionality and decision support. *Nucleic Acids Research*, gkae236. <https://doi.org/10.1093/nar/gkae236>

21. Chen, X., Li, H., Tian, L., Li, Q., Luo, J., & Zhang, Y. (2020). Analysis of the physicochemical properties of acaricides based on Lipinski's rule of five. *Journal of computational biology*, 27(9), 1397-1406. <https://doi.org/10.1089/cmb.2019.0323>
22. Sucharitha, P., Reddy, K. R., Satyanarayana, S. V., & Garg, T. (2022). Absorption, distribution, metabolism, excretion, and toxicity assessment of drugs using computational tools. In *Computational approaches for novel therapeutic and diagnostic designing to mitigate SARS-CoV-2 infection* (pp. 335-355). Academic Press. <https://doi.org/10.1016/B978-0-323-91172-6.00012-1>
23. Wang, Y., Xing, J., Xu, Y., Zhou, N., Peng, J., Xiong, Z., ... & Jiang, H. (2015). *In silico* ADME/T modelling for rational drug design. *Quarterly reviews of biophysics*, 48(4), 488-515. <https://doi.org/10.1017/S0033583515000190>
24. Daoud, N. E. H., Borah, P., Deb, P. K., Venugopala, K. N., Hourani, W., Alzweiri, M., ... & Tiwari, V. (2021). ADMET profiling in drug discovery and development: perspectives of *in silico*, *in vitro* and integrated approaches. *Current Drug Metabolism*, 22(7), 503-522. <https://doi.org/10.2174/1389200222666210705122913>
25. Kehinde, O. A. Q., Damilare, B. I., Ogunlana, A., Mojeed Ayoola, A., Opeyemi Emmanuel, A., & Temitope Isaac, A. (2022). Inhibitors of α -glucosidase and Angiotensin-converting Enzyme in the Treatment of Type 2 Diabetes and its Complications: A Review on *in silico* Approach. *Pharmaceutical and Biomedical Research*, 8(4), 237-258. <http://dx.doi.org/10.32598/PBR.8.4.1052.1>
26. Oyedele, A. Q. K., Adelusi, T. I., Ogunlana, A. T., Adeyemi, R. O., Atanda, O. E., Babalola, M. O., ... & Boyenle, I. D. (2022). Integrated virtual screening and molecular dynamics simulation revealed promising drug candidates of p53-MDM2 interaction. *Journal of Molecular Modeling*, 28(6), 142. <https://doi.org/10.1007/s00894-022-05131-w>
27. Eberhardt, J., Santos-Martins, D., Tillack, A. F., & Forli, S. (2021). AutoDock Vina 1.2. 0: New docking methods, expanded force field, and python bindings. *Journal of chemical information and modeling*, 61(8), 3891-3898. <https://doi.org/10.1021/acs.jcim.1c00203>
28. Fikes, A. G., & Srougi, M. C. (2023). Design and Implementation of an Accessible and Open-Sourced *In silico* Drug Screening Activity for Cancer Drug Discovery. *Journal of Chemical Education*, 100(10), 4125-4130. <https://doi.org/10.1021/acs.jchemed.3c00307>
29. Ehigie, L. O., Ojeniyi, F. D., Rashidat, A., Igbeneghu, C., Sulaimon, N., & Ehigie, A. F. (2022). Molecular Docking and Molecular Dynamics Simulation to Investigate Protein-Ligand Binding of Potential Drug Candidates from *Vernonia Amygdalina* Against Wilms'tumor 1 (Wt1) Protein. *European Journal of Biomedical*, 9(8), 499-514. Issn 2349-8870
30. Olaniyan, L. W. B., Ehigie, L. O., Ehigie, A. F., Emmanuel, O., Atanda, T. T. O., & Fakuade, A. A. (2024). *In silico* Investigation of Indenoimidazole Derivatives as Promising Arsenal Against

- Methicillin Resistant Staphylococcus Aureus Through Staphylococcal Protein A Inhibition. *European Journal of Biomedical*, 11(6), 04-16. Issn 2349-8870
31. Babalola, M. O., Ashiru, M. A., Boyenle, I. D., Atanda, E. O., Oyedele, A. Q. K., Dimeji, I. Y., ... & Imaga, N. A. (2022). In vitro Analysis and Molecular Docking of Gas Chromatography-Mass Spectroscopy Fingerprints of Polyherbal Mixture Reveals Significant Antidiabetic Mixture. *Nigerian Journal of Experimental and Clinical Biosciences*, 10(4), 105-115. https://doi.org/10.4103/njecp.njecp_15_22
 32. Ajao, F. O., Ehigie, A. F., Odunitan, T. T., Atanda, O. E., Ayoola, P. B., & Olaniyan, L. W. (2024). Computational Exploration of Psidium guajavae Folium Bioactive Compounds As Novel Dpp-iv Inhibitors For Type 2 Diabetes Mellitus Intervention. Issn 2394-3211
 33. Genheden, S., & Ryde, U. (2015). The MM/PBSA and MM/GBSA methods to estimate ligand-binding affinities. *Expert opinion on drug discovery*, 10(5), 449-461. <https://doi.org/10.1517/17460441.2015.1032936>
 34. Virtanen, S. I., Niinivehmas, S. P., & Pentikäinen, O. T. (2015). Case-specific performance of MM-PBSA, MM-GBSA, and SIE in virtual screening. *Journal of Molecular Graphics and Modelling*, 62, 303-318. <https://doi.org/10.1016/j.jmgm.2015.10.012>
 35. Shukla, R., & Tripathi, T. (2020). Molecular dynamics simulation of protein and protein–ligand complexes. *Computer-aided drug design*, 133-161. https://doi.org/10.1007/978-981-15-6815-2_7
 36. Elz, A. S., Trevaskis, N. L., Porter, C. J., Bowen, J. M., & Prestidge, C. A. (2022). Smart design approaches for orally administered lipophilic prodrugs to promote lymphatic transport. *Journal of Controlled Release*, 341, 676-701. <https://doi.org/10.1016/j.jconrel.2021.12.003>
 37. Han, S., Mei, L., Quach, T., Porter, C., & Trevaskis, N. (2021). Lipophilic conjugates of drugs: a tool to improve drug pharmacokinetic and therapeutic profiles. *Pharmaceutical Research*, 38(9), 1497-1518. <https://doi.org/10.1007/s11095-021-03093-x>
 38. Costliow, Z. A. (2018). *Identification and characterization of thiamine biosynthesis, transport, and regulation elements among bacteroides species* (Doctoral dissertation, University of Illinois at Urbana-Champaign). <http://hdl.handle.net/2142/102879>
 39. Zhang, A., Meng, K., Liu, Y., Pan, Y., Qu, W., Chen, D., & Xie, S. (2020). Absorption, distribution, metabolism, and excretion of nanocarriers in vivo and their influences. *Advances in Colloid and Interface Science*, 284, 102261. <https://doi.org/10.1016/j.cis.2020.102261>
 40. AlRawashdeh, S., Chandrasekaran, S., & Barakat, K. H. (2023). Structural analysis of hERG channel blockers and the implications for drug design. *Journal of Molecular Graphics and Modelling*, 120, 108405. <https://doi.org/10.1016/j.jmgm.2023.108405>
 41. Malik, D., Narayanasamy, N., Pratyusha, V. A., Thakur, J., & Sinha, N. (2023). Water-Soluble Vitamins. In *Textbook of Nutritional Biochemistry* (pp. 291-389). Singapore: Springer Nature Singapore. https://doi.org/10.1007/978-981-19-4150-4_10

42. Spassov, D. S. (2024). Binding Affinity Determination in Drug Design: Insights from Lock and Key, Induced Fit, Conformational Selection, and Inhibitor Trapping Models. *International Journal of Molecular Sciences*, 25(13), 7124. <https://doi.org/10.3390/ijms25137124>

UNDER PEER REVIEW